Parameterized Wildfire Fragility Functions for Overhead Power Line Conductors

Mostafa Nazemi, *Member, IEEE*, Payman Dehghanian, *Senior Member, IEEE*, Yousef Darestani, and Jinshun Su, *Graduate Student Member, IEEE*

***Abstract*—Wildfires have been, recently more-frequently, posing significant threats to the safety and reliability of electric power delivery infrastructure, calling for the development of dedicated risk and vulnerability assessment frameworks. Fragility functions are essential tools for probabilistic risk assessment to estimate the failure likelihood of the system components as a function of hazard intensity. Widely exposed to the environment and atmospheric stressors, overhead power line conductors are among the most susceptible electric delivery infrastructure to approaching wildfires. Beyond the state-of-the-art fragility models, this article proposes novel parameterized wildfire fragility functions that can capture the impact of different environmental conditions and wildfire severity measures on overhead power line conductors. In doing so, wildfire behaviour is comprehensively characterized in order to model the temperature change in overhead conductors in the face of progressing wildfires. A novel parametric fragility model, which is a function of a set of physical and environmental features (e.g., conductor height, landscape slope, the dryness of fuel, fuel depth, wind speed, flame length), is then suggested to assess the failure likelihood of conductors given a permissible safety conductor temperature rise. A set of fire features (e.g., fire line intensity, fire rate of spread, and the angle of the fire approaching the conductors) is embedded in the proposed fragility model to capture the wildfire uncertainties. The numerical results reveal that, unlike the commonly-used fragility models, the proposed parameterized fragility function is able to accurately represent the impact of critical physical, environmental, and fire features in determining the vulnerability of power distribution lines when facing wildfire emergencies.**

***Index Terms*—Wildfire hazards, parameterized fragility functions, risk assessment, power distribution systems, overhead power line conductors.**

Manuscript received 2 June 2022; revised 30 January 2023 and 11 May 2023; accepted 11 July 2023. Date of publication 25 July 2023; date of current version 21 February 2024. This work was supported by the National Science Foundation (NSF) under Grant ECCS-2114100, Grant RISE-2022505, and Grant RISE-2220626. Paper no. TPWRS-00793-2022. *(Corresponding author: Payman Dehghanian.)*

Mostafa Nazemi is with the MPR Associates, Inc., Alexandria, VA 22314 USA (e-mail: mnazemi@mpr.com).

Payman Dehghanian and Jinshun Su are with the Department of Electrical and Computer Engineering, George Washington University, Washington, DC 20052 USA (e-mail: payman@gwu.edu; jsu66@gwu.edu).

Yousef Darestani is with the Department of Civil, Environmental, and Geospatial Engineering, Michigan Technological University, Houghton, MI 49931 USA (e-mail: ydaresta@mtu.edu).

Color versions of one or more figures in this article are available at https://doi.org/10.1109/TPWRS.2023.3298769.

Digital Object Identifier 10.1109/TPWRS.2023.3298769

I. Introduction

A. Motivation and Rationale

THE world has been witnessing more-frequent higher-intensity wildfire incidents resulting in death, massive economic losses, and the destruction of facilities and assets. Over 200,000 wildfire incidents were reported in the United States between 2017 and 2020, scorching over 25 million acres [1]. Only between January and July 2020, there were over 27,770 wildfires that torched over 1.7 million acres. Due to climate change and global warming, and with the resulting dryness and drought conditions, fire seasons have been observed to start earlier and last longer [2]. By mid-2021, California's drought situation had already witnessed a 26% spike in wildfire incidents and a 58% increase in burnt landscape compared to 2020, putting the state on track for another record-breaking year [3]. This year-over-year increase in wildfire risk has reached a tipping point which calls for new solutions for enhanced situational awareness and informed asset inspections to ensure reliable and resilient delivery of electricity to the end-use consumers.

Power distribution systems are particularly vulnerable to wildfire risks, where overhead power lines are routed through fire-prone geographical regions with dense vegetation. The pole—which is often made of wood, the overhead conductor, and the insulator are the three basic components of a power distribution line. In case of an intensive fire, it is likely that the wood pole would catch fire and the conductor would melt. There are, however, several minor to moderate wildfires with varying flame lengths that might cause thermal stress on the overhead power line conductors [4]. The increased temperature of the conductor produced by wildfires may compromise ground clearance owing to sag. The conductor also may lose its ultimate tensile strength when exposed to high temperature [5]. In addition, annealing a conductor will cause line failure under heavy loads [6]. Therefore, the resulting thermal stress on overhead power line conductors must be included in failure risk evaluations and reliability analysis of power distribution conductors to ensure a safe and desired operation.

B. Literature Review

Several studies have investigated the impact of heat stress on the mechanical strength of Aluminum Conductor Steel Reinforced (ACSR) power distribution lines. The annealing properties of the aluminum component of ACSR due to thermal

overloading were first analyzed in [7]. In [8] investigates the mechanical characteristics of ACSR conductors in the presence of forest fires. To assess the failure probability of the ACSR-type power lines near a large-scale jet fire of ruptured high-pressure gases, a thermal failure model is provided in [9] and a new approach is used for heat transmission from jet fires as well as a distribution model for conductor failure probability. In [10] explores how fire conditions alter ACSR-type conductors, inducing elongation of the lines and underlying vegetation. Estimation of thermal energy transmitted to an object from a wildfire is more complicated due to the complex interactions of the landscape features, e.g., fuel depth, slope, type of vegetation, and meteorological conditions, e.g., wind speed, wind direction, ambient temperature [11]. A comprehensive model is introduced in [4] that estimates the temperature rise (and not the failure likelihood) of the power line conductors with some knowledge on the fire characteristics.

Focused on the aftermath of fires, in [12] develops an optimization framework for mitigating wildfire disruptions in power grids capturing its spatiotemporal behavior and characteristics. Dynamic line rating of overhead conductors is considered in [13] to determine the optimal resilient operation of a power grid exposed to an approaching wildfire. Through applying dynamic heat balance equations to evaluate the temperature rise of overhead conductors, a study in [14] proposes an optimization framework for resilient operation and optimal coordination of local energy sources during wildfire incidents. The study in [15] introduces a probabilistic proactive generation re-dispatch strategy to boost the operational resilience of power grids during wildfires by capturing the propagation properties and spatiotemporal characteristics of wildfires.

Additionally, some references use the fragility concept to determine power system component failure likelihoods during adverse weather events. In [16] develops a resilience assessment framework with a computational algorithm to evaluate the response of the power grid during hurricane incidents. The framework quantifies the performance of electrical components against hurricanes via a fragility function solely driven by wind speed. With the application of fragility assessment methodologies, the study in [17] introduces a stochastic approach to prioritize the inspection timeline of aging wood poles. A stochastic modeling approach involving hurricane hazard, component fragility, power system performance, and system restoration models is presented in [18]. In [19] provides a set of multi-dimensional fragility functions to estimate risk and perform cost analysis for wood utility poles under wind hazards. A set of parameterized fragility functions capturing multi-hazard effects along with the utility pole's failure modes is proposed in [20].

C. Problem Statement and Contribution

Previous studies on electrical infrastructure risk analysis have mainly focused on simple empirical fragility models which solely predict the failure likelihood of transmission towers, distribution poles, and overhead power line conductors as a function of one single parameter, e.g., age of wood pole [21] and wind speed [16], [17], [18], [22], [23], [24]. In the case of wildfires, employing such one-dimensional fragility curves may not accurately represent the likelihood of failure due to the complex interactions of *physical features*, *environmental features*, and *fire features*. Physical and environmental features usually refer to a set of quantities that can be directly determined and measured (e.g., wind speed, fuel depth, and conductor height). Fire features refer to those parameters that are difficult to calculate or are naturally characterized with uncertainties (e.g., fire rate of spread or fire line intensity).

To the best of our knowledge, there is no existing wildfire fragility model in the literature for power line conductors. To fill in the knowledge gap, we introduce a novel parameterized wildfire fragility model that takes into account the complex relationships among physical, environmental, and fire features, providing dynamic estimates of the likelihood of failure for overhead power line conductors as wildfires progress. This contributes to a better understanding of the interplay impact of these factors on the conductors' failure likelihood during wildfires. An efficient logistic regression model is applied to construct a closed-form expression for the likelihood of failure of overhead power line conductors in the face of progressing wildfires, where various environmental features are intertwined with fire uncertainties. This article aims to serve as a starting point in the literature to develop multi-dimensional wildfire fragility models that surpass the limitations of the simple one-dimensional empirical fragility models commonly relied on in previous research.

The rest of the article is organized as follows. Section II employs the wildfire heat transfer model to determine the rise in temperature of overhead power line conductors in the face of progressing wildfires. The parameterized wildfire fragility functions for ACSR-type conductors are introduced in Section III. Numerical case study and simulation results are presented and discussed in Section IV. Section V illustrates the application of the proposed fragility function in a power distribution system facing an approaching wildfire. The article is eventually concluded in Section VI.

II. Temperature Rise Estimation of the Overhead Power Line Conductors

A. Background

In the United States, ACSR composite conductors are favored for use in power distribution systems due to their economic viability and mechanical robustness. In case of wildfires, three forms of heat transferred to an object may be distinguished: *conduction*, *convection*, and *radiation*. Thermal conduction is the flow of internal energy through small particle collisions and electron movement within a substance. Thermal convection is the transfer of energy through fluid motion. Thermal radiation is related to energy transmission via electromagnetic waves. Conduction type of heat transmission only contributes to an increased conductor temperature when the fire directly contacts the conductor, which occurs when the flame height is substantial. This article only considers fires with small to moderate flame length, i.e., 10 cm to 4 m, as more intense wildfires will most likely burn the wood pole and will melt the conductor. Therefore,

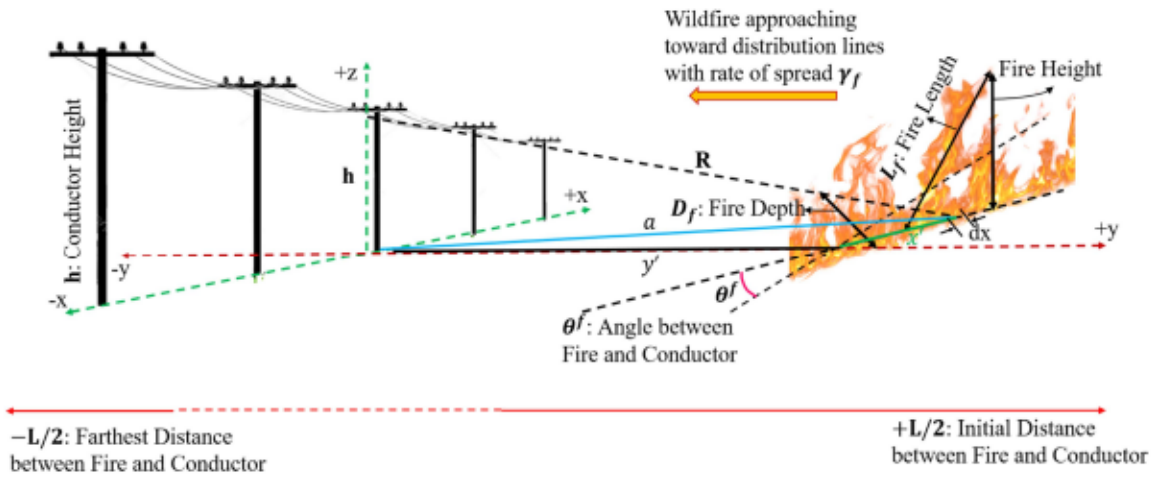

Fig. 1. Representation of parameters for a wildfire approaching toward overhead power distribution line conductors.

only convection and radiation forms of heat transmission are here considered [4]. Note that heat transmission through convection tends to flow upward because hot air rises. During wildfires, burning materials on the land cause convection currents, which warm anything above the fire. Therefore, convection heat transferred from wildfire to the conductor can only contribute to an increased conductor temperature when the fire is exactly under the conductor.

B. Conductor Temperature Change Model

Based on the wildfire model presented in [4], we calculate the value of the temperature rise in ACSR-type overhead conductors exposed to approaching wildfires. Fig. 1 presents several parameters that will be used to characterize the conductor temperature change model. The fire rate of spread γ_f (m/s) can be accordingly assessed as [25]:

$$\gamma_f = 0.773 V_w^{0.707}.\exp(0.062S - 0.039M_s)F_D^{0.188}, \quad (1)$$

where V_w indicates wind speed (m/min), S represents the landscape slope (°), M_s states the fuel aridity index (%), and F_D indicates the fuel depth (cm).

Considering D_f (m) as the fire depth, the time during which the fire is passing under the conductor is D_f/γ_f. Derived from the convective heat equation (see Appendix A), the following (2) can be used to compute the conductive heat energy W_c (kJ/m^2) when the fire is right beneath the overhead power line conductor:

$$W_c = 22.C_f.\frac{D_f}{\gamma_f}.\sqrt[3]{\frac{I_B^2}{h^5}}, \quad (2)$$

where I_B is the fire line intensity (kW/m) and can be calculated as follows [25]:

$$I_B = 185.2.L_f^{1.842}, \quad (3)$$

where L_f represents the length of fire (m).

Considering the wildfire approaches the conductor with the rate of spread γ_f and the distance that fire passes through is from $(+l/2)$ to $(-l/2)$ on the y axis, the radiative heat energy W_r (kJ/m^2) can be presented as follows (see Appendix B for more detail):

$$W_r = \frac{I_B.\cos\theta}{10.\gamma_f}.\left[\ln\left(\frac{l}{h}\right) + \ln\left(1+\sqrt{1+\left(\frac{h}{l}\right)^2}\right)\right]. \quad (4)$$

As discussed in Section II-A, the total heat energy W_T (kJ/m^2) transferred from wildfire to the conductor surface is the summation of conductive heat energy and radiative heat energy as follows:

$$W_T = W_c + W_r \quad (5)$$

Focusing on the ACSR-type overhead line conductors, the temperature rise of the conductor in the face of wildfires can be obtained as [26]:

$$\Delta\Theta = \frac{4.W_T.d_c}{\pi.(\varkappa_{st}.\varsigma_{st}.\omega_{st}.\pi.\delta_{st}^2 + \varkappa_{Al}.\varsigma_{Al}.\omega_{Al}.\pi.\delta_{Al}^2)}, \quad (6)$$

The definition and the value of each parameter in the above equation are explained in Table VII in Appendix C.

III. The Proposed Parameterized Fragility Function for Overhead Power Line Conductors

A. Overview

The temperature rise of the ACSR-type overhead line conductors under a wildfire event depends on a set of physical, environmental, and fire features. In this study, physical features are defined by a set of quantities that can be easily determined and measured from the conductor configuration. The sample spaces of such features are characterized uniformly in the experiment designed for the proposed fragility function. With the same sample space characteristics as physical features, environmental features refer to some parameters that help evaluate the hazard severity, such as wind speed and flame length. Since the Halton quasi-random point set is an efficient sampling method on a probabilistic space following a uniform distribution [27], we utilize the Halton quasi-random point set to generate realizations

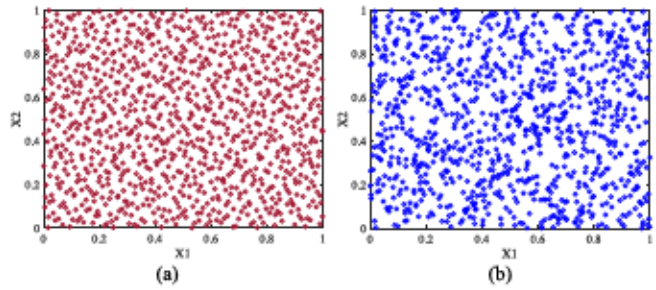

Fig. 2. Design space generated by (a) the Halton Quasi-Random point method, and (b) the LHS method.

of physical and environmental features for the proposed fragility function.

The proposed fragility function also captures fire features which are uncertain parameters due to epistemic (lack of knowledge) or aleatory (natural randomness) uncertainty. Furthermore, fire features such as fire intensity or rate of spread are stochastic and nonlinear in nature, making it difficult to capture their dynamics. Due to the dense and efficient stratification across the range of each random variable, LHS is effective in sensitivity analysis and model verification [28]. Compared with random sampling and fast probability integration sampling, LHS is more stable (i.e., less variation in estimated distribution functions from sample to sample) for sampling uncertain parameters [28]. Therefore, the LHS technique is employed to generate realizations of fire features that follow a specific distribution. It should be noted that there are indeed a variety of ways introduced in the literature to generate the training points including the LHS method, the Centroidal Voronoi Tessellation (CVT) method [29], and the Halton quasi-random point set. While the CVT technique provides consistent coverage of the design space, it is computationally demanding for problems with a large number of training points and high dimensionality. The LHS approach, on the other hand, is not computationally intensive but does not yield a design space with consistent coverage for high-dimensional inputs. Fig. 2 compares the LHS with Halton quasi-random point set techniques for a set of two physical features ranging between zero to one per unit. One can realize that the LHS approach does not perform as well as the Halton method because the generated sample space produced by LHS usually includes numerous empty patches, whereas the Halton technique provides a much more consistent design space.

B. Failure Mode of Overhead Line Conductors

According to electric utilities [30] and [31], a continuous operating temperature range of 75 $^{\circ}C$ is considered for ACSR-type bare overhead conductors. ACSR-type conductors have an industry-accepted maximum operation temperature rating of 100 $^{\circ}C$. Operating at maximum temperature can cause substantial damages to the conductor, such as an increase in conductor sag or a decrease in conductor tensile strength. Therefore, the following equation characterizes the failure or survival mode of the overhead line conductors when facing wildfire incidents.

$$\mathbf{F}(X_{r,d}) = \Delta\Theta(X_{r,d}) - 25^{\circ} \tag{7}$$

TABLE I
PHYSICAL AND ENVIRONMENTAL FEATURES IN THE PROPOSED FRAGILITY FUNCTION [25]

Features	Notation	Min	Max
Slope (°)	S	-6	17
Fuel Aridity Index (%)	M_s	3.7	41.7
Fuel Depth (cm)	F_D	0.1	5.5
Conductor Height (m)	h	6.1	38.1
Wind Speed (km/h)	V_w	0.5	80.47
Flame Length (m)	L_f	0.1	4.2

TABLE II
FIRE FEATURES IN THE PROPOSED FRAGILITY FUNCTION

Features	Notation	Distribution [Min Max] / (μ SD)*
Fire Path Length (m)	l	Uniform [1 30]
Angle between Fire and Conductor (°)	θ	Uniform [0 90]
Air Heat Coefficient ($\frac{kW}{m^2.^{\circ}K}$)	C_F	Normal (0.06 0.01)

* μ and SD reflect the mean and standard deviation of normal distribution.

The failure mode of the conductor is defined if the conductor temperature rise is more than 25 $^{\circ}C$ assuming that the normal operating temperature of the conductor in a sunny day and in full capacity is 75 $^{\circ}C$. X_r denotes the contribution of the fire features to the temperature rise and X_d refers to the physical/environmental features of wildfires.

C. Parameterized Fragility Functions

As mentioned previously, the wildfire fragility function developed in this study is based on a set of physical, environmental, and fire features. According to (1)–(4), *physical features* involve landscape slope, fuel aridity index, fuel depth, and conductor height, while *environmental features* are wind speed and flame length. The list of physical and environmental features along with their associated minimum and maximum values are presented in Table I. *Fire features* include fire path length, air heat coefficient, as well as the angle between fire and the conductor, which are presented in Table II with the information on their specific distributions.

To develop parameterized fragility functions, a set of 20,000 training points for each single physical and environmental feature are generated using the Halton quasi-random point set. The LHS technique is employed to generate 20,000 realizations for each uncertain parameter corresponding to fire features. The samples generated by Halton and LHS techniques are integrated into one giant data pool where one binary variable ω, representing the failure and survival mode of overhand conductors, is assigned to each realization to evaluate the failure likelihood of overhead conductors at each data point based on (7).

$$\omega := \begin{cases} 0 & \text{if } \mathbf{F}(X_{r,d}) < 0 \\ 1 & \text{if } \mathbf{F}(X_{r,d}) \geq 0 \end{cases} \tag{8}$$

where $\omega = 0$ denotes the survival mode, and $\omega = 1$ indicates a failure mode. If the response outcome is binary, logistic regression can be suitably utilized to estimate the occurrence likelihood

Algorithm 1: The Proposed Parameterized Wildfire Fragility Algorithm for Overhead Power Line Conductors.

1: Generate n samples for X_d using the Halton technique
2: Generate n samples for X_r using the LHS technique
3: Define K as set of all realizations of X_r and X_d
4: **for all** $k \in K$ **do**
5: Initialize $\vartheta_k = 0$, $\mathbf{F}(X_{r,d}) = 0$, and $\omega_k = 0$
6: Calculate $\Delta\Theta(X_{r,d})$ based on (6)
7: $\vartheta_k \leftarrow \Delta\Theta(X_{r,d})$
8: $\mathbf{F}(X_{r,d}) \leftarrow \vartheta_k - 25$
9: **if** $\mathbf{F}(X_{r,d}) \geq 0$ **then**
10: $\omega_k = 1$
11: **else**
12: $\omega_k = 0$
13: **end if**
14: **end for**
15: Run the logistic regression model based on values of ω_k
16: Obtain the coefficients of (10)
17: **Output:** $\mathbf{P}(\mathbf{failure}|S, M_s, F_D, h, V_w, L_f)$

of an event [32]. A logistic regression model is developed to obtain the failure likelihood of the conductors given the specific physical and environmental features as follows:

$$\mathbf{P}(\mathbf{failure}|S, M_s, F_D, V_w, h, L_f) = \frac{1}{1 + \exp\left[-\ell(S, M_s, F_D, V_w, h, L_f)\right]} \tag{9}$$

where $\ell(S, M_s, F_D, h, V_w, L_f)$ is the logarithm of the odds which can be represented in the following format.

$$\ell(S, M_s, F_D, h, V_w, L_f) = a_0 + a_1(S) + a_2(M_s) + a_3(F_D) + a_4(V_w) + a_5(h) + a_6(L_f) \tag{10}$$

The coefficients a_0 to a_7 can be obtained using the logistic regression over 20,000 generated samples for physical, environmental, and fire features. Algorithm 1 summarizes the proposed process to achieve the failure likelihood of overhead line conductors given a set of physical and environmental features as stated in model (9).

IV. Numerical Results

The proposed fragility model (9) which is a function of 6 dimensions, i.e., *slope*, *fuel aridity index*, *fuel depth*, *conductor height*, *wind speed*, and *flame length* is generated and numerically investigated in this Section. We used MATLAB R2021b software platform to conduct all studied tests experimented on a PC with an Intel i7-8700 processor and 32 GB RAM.

A. Model Evaluation

Each corresponding coefficients used in the failure likelihood expression (10) are estimated in Table III using the logistic regression model. It should be noted that *p-value* reflects the importance of each coefficient, highlighting that the closer the value is to zero and less than 0.05, the more significant the coefficient will be. Since logistic regression is a classification model, the area under Receiver Operation Characteristics (ROC) curve is here utilized to assess the goodness of fit for the suggested regression approach [20]. ROC curve is a graphical plot that validates the ability of a binary classifier (i.e., the logistic regression model) with varied discrimination thresholds [33]. This curve is constructed by graphing the true positive rate (sensitivity) vs. the false positive rate (specificity) at various threshold levels. In ROC curve, the closer both sensitivity and specificity are to 1, the better the performance of the classification method. As shown in Fig. 3, the area under the ROC curve gets a value between 0.5 (which represents the random classifier) and 1 (which represents the perfect classifier). In order to validate the accuracy of the proposed parameterized wildfire fragility functions, the ROC curve for the model (9) is provided in Fig. 3 (i.e., red solid line). The area under the ROC curve is equal to 0.9088, which indicates that the logistic regression model in this study is highly accurate. In this study, the number of samples for X_d, and X_r were increased from 5,000, 10,000, and 20,000, 30,000 in order to conduct a convergence study. Due to the insignificant difference in the results when experimenting 20,000 and 30,000 samples, the values listed in Table III are generated based on the experiment with 20,000 number of samples.

TABLE III
The Coefficients in the Failure Likelihood Function Characterized Using the Logistic Regression Model

Coefficients	Estimate	p-value
Intercept	-0.5417	0.000
a_1	-0.1101	0.000
a_2	0.066312	0.000
a_3	-0.13069	0.000
a_4	-0.040483	0.000
a_5	-0.084872	0.000
a_6	1.7325	0.000

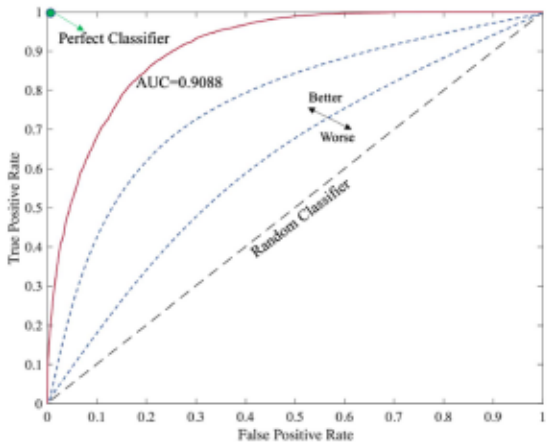

Fig. 3. Area under the ROC curve for the studied logistic regression case.

B. Sensitivity Analysis

Fig. 4 illustrates the generated 20,000 samples, which were classified into two categories (failure vs. not failure) in order to

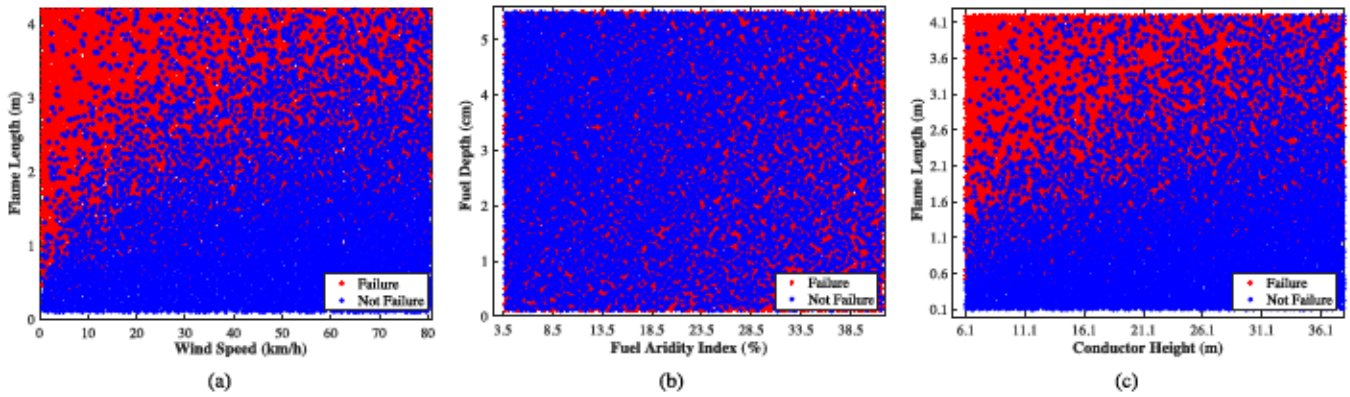

Fig. 4. Sensitivity analyses conducted for 20 000 generated random samples: (a) wind speed vs. flame length, (b) fuel aridity index vs. fuel depth, and (c) conductor height vs. flame length.

TABLE IV
PARAMETERS OF THE FRAGILITY CURVES IN FIG. 5

Fig.	Parameters					
	S (°)	M_s (%)	F_D (cm)	V_w (km/h)	h (m)	L_f (m)
5a	0	10	3	5–75	15	-
5b	-	10	3	5–75	15	0.5
5c	0	10	-	5–75	15	0.5
5d	0	-	3	5–75	15	0.5
5e	0	10	3	40	-	0.25–4
5f	-6–17	10	3	-	15	0.5

analyze the conductor failure possibilities under four random parameters. Firstly, One can realize from Fig. 4(a) that the failure scenario occurs most likely when the wind speed is not very strong, i.e., $V_w \leq 20\ km/h$ and the flame length is more than 1 m. This observation is because according to (1), the slower wind speed leads in a reduced fire rate of spread giving the conductor more time to absorb both W_c and W_r—(2) and (4)—resulting in higher conductor temperature. Secondly, Fig. 4(b) demonstrates that the dryer the fuel is, the more severe the wildfire would be regardless of the fuel depth which results in more failure scenarios. One can notice that fuel depth—which is assumed to vary between 0.1 to 5.5 cm—has minor impact on the conductor failure. Eventually, one can see from Fig. 4(c) that the taller conductors are less at risk of failure by wildfires. It can also be realized that for flame lengths more than 2.5 m, the wildfire will be highly severe, resulting in failure scenarios less dependent on the conductor height.

Fig. 5 represents the fragility curves of the overhead power line conductors in the face of an approaching wildfire considering 6 different dimensions: *length of fire*, *slope*, *fuel depth*, *fuel aridity index*, *conductor height*, and *wind speed*. In Fig. 5(a)–(d), the likelihood of conductor failure, i.e., when the probability of conductor temperature increment is found greater than 25 °C, is obtained for different wind speed scenarios, whereas the failure likelihood is investigated in Fig. 5(e) and (f) for different scenarios of flame length and slope, respectively. The physical features that are used to achieve each 2-dimensional fragility curve in Fig. 5 are tabulated in Table IV. One can realize from Fig. 5(a)–(d) that the slower wind speed results in a higher failure likelihood since, according to (1), slower wind speed leads to slower fire rate of spread giving the conductor more time to absorb both W_c and W_r—see (2) and (4), resulting in a higher rise in the conductor temperature. Fig. 5(a) reveals that the length of fire, as a severity measure of wildfire, has a substantial influence on the conductor temperature rise since severe wildfires with high intensity typically have longer flame lengths, which can exceed 4 meters in our examined example. Considering negative slopes for downhill landscapes, zero slope for flat landscapes, and positive slopes for uphill landscapes, Fig. 5(b) illustrates that fire can grow quicker and become a massive one for negative slopes, increasing the likelihood of conductor failure. Fig. 5(c) shows that it is likely to see that the failure likelihood varies slightly depending on the fuel depth. The deeper the fuel depth, the more impurity may be contained, resulting in a smaller fire and a lesser likelihood of failure. On the other hand, one can see from Fig. 5(d) that the dryer the fuel, the bigger the fire, leading to a higher failure likelihood. In the face of impending fires, taller conductors had a substantially lower likelihood of failure than shorter ones, according to Fig. 5(e). For example, the failure likelihood for taller conductors, e.g., with the height of 20 m to 38 m, is less than 10% for flames with a length of less than 1 m. Fig. 5(f) demonstrates that as wind speed increases, the likelihood of failure decreases dramatically. Furthermore, for negative slopes, fires might have a significant influence on the failure likelihood. For instance, for wind speed of 20 km/h, the likelihood of failure varies between 4% and 28% for slope of 15° and −5°, respectively.

Fig. 6 illustrates three-dimensional fragility curves of overhead power line conductors. One can realize from Fig. 6(a) that an increase in the flame length and a decrease in the conductor height result in a higher failure likelihood. For instance, for flame length of 2.6 m, if the conductor height changes from 11 m to 28 m, the failure likelihood decreases from 0.84303 to 0.55925. According to Fig. 6(b), it can also be shown that the flame length and fuel aridity index have a significant impact on the conductor's likelihood of failure. For example, Fig. 6(b) shows that for a flame length of 1.7 m, increasing the fuel aridity index from 17% to 30% raises the likelihood of overhead power line failure from 0.56129 to 0.75184.

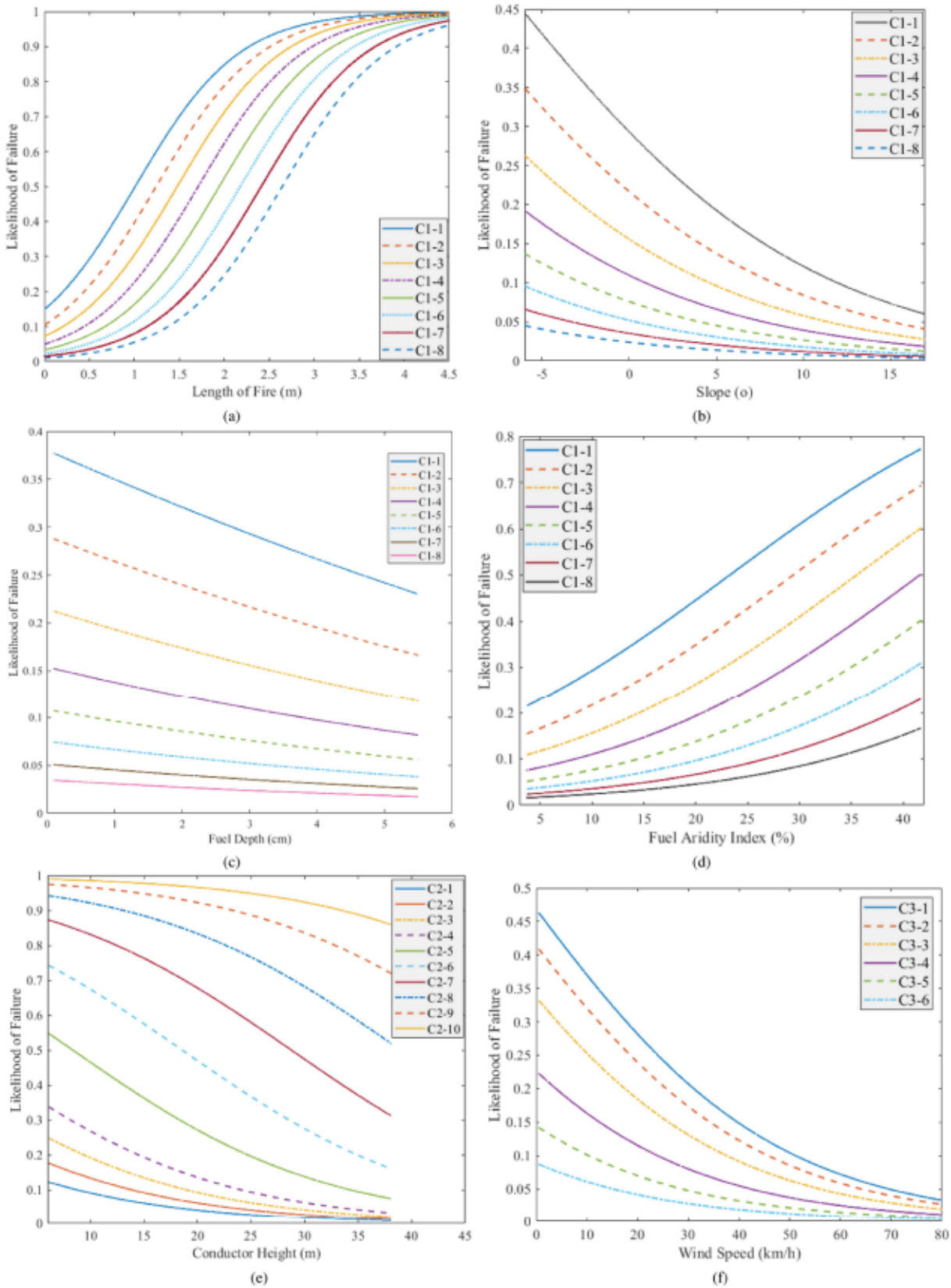

Fig. 5. Parameterized fragility curves for overhead power line conductors: (a) Likelihood of failure given the length of fire, (b) likelihood of failure given the slope of landscape, (c) likelihood of failure given the fuel depth, and (d) likelihood of failure given the fuel aridity index for different wind speed cases with 10 km/h increments (C1-1=5 km/h to C1-8=75 km/h); (e) likelihood of failure given the conductor height for different flame length cases (C2-1=0.25 m, C2-2=0.5 m, C2-3=0.75 m, C2-4=1 m, C2-5=1.5 m, C2-6=2 m... C2-10=4 m); and (f) likelihood of failure given wind speed for different slopes (C3-1=-5°, C3-2=-3°, C3-3=0°, C3-4=5°, C3-5=10°, C3-6=15°).

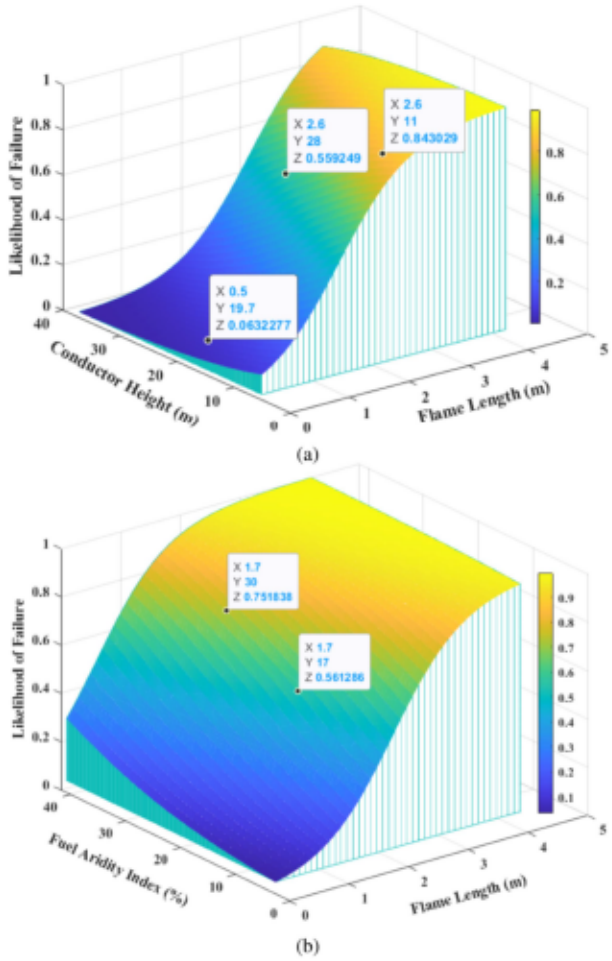

Fig. 6. Three-dimensional fragility curves to estimate the failure likelihood of overhead conductors given: (a) flame length and conductor height, and (b) flame length and fuel aridity index.

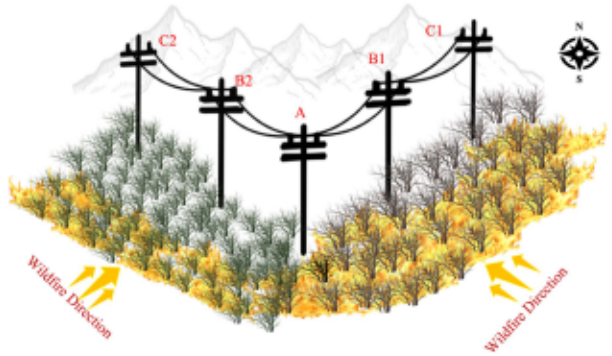

Fig. 7. Two Different wildfire scenarios approaching overhead conductors A-B1-C1 and A-B2-C2 in a power distribution grid.

V. Application of the Proposed Fragility Models in Wildfire-Attacked Power Distribution Systems

The suggested parameterized fragility curves can be used by power distribution system operators to estimate the vulnerability of overhead power lines in the face of wildfire incidents. Fig. 7 depicts two sets of overhead power line conductors and two distinct pathways wildfires take to reach the conductors. To evaluate the likelihood of failure of conductors dynamically, five different sample time periods are assumed when the fires approach the power lines. It is also considered that the type of vegetation, the aridity index of vegetation, the fuel depth, the landscape slope, the wind speed, and the flame length vary at each different time period. One can realize from Tables V and VI that the set of overhead conductors A-B1-C1 has a substantially greater failure likelihood than conductors A-B2-C2 because the evaluated physical and environmental features for flames approaching conductors A-B1-C1 result in a more intense wildfire. For instance, at t_2, a negative slope of -4° with a fuel aridity index of 20% is far more likely to yield a larger fire near conductors A-B1-C1 than a positive slope of $+12^\circ$ with a fuel aridity index of 3% for flames approaching conductors A-B2-C2. It should also be noted that, while the flame length does play a significant role in the likelihood of conductor failure, longer flames do not necessarily result in a higher failure likelihood. For example, Table VI reveals that despite the fire flame length is 0.5 m longer at t_5 than it was at t_4, the likelihood of failure is 6.21% lower. As a result, various criteria such as wind speed, fuel aridity index, terrain slope, etc. must be jointly considered in order to precisely assess the conductor's increased temperature and its failure likelihood. A performance comparison between the proposed parameterized wildfire fragility model and the existing alternatives is presented in Appendix D. This clearly highlights the underlying rationale and emphasizes the need for employing the suggested parameterized wildfire fragility models for overhead power line conductors rather than the existing practice often relying on the conservative two-dimensional fragility models.

TABLE V
Parameters for a Wildfire Approaching Overhead Conductors A-B2-C1 and the Associated Time-Variant Failure Likelihood

Time	Physical/Environmental Features						P(Failure)
	S (°)	M_s (%)	F_D (cm)	V_w (km/h)	h (m)	L_f (m)	
t_1	10	5	1	10	15	0.3	**0.0691**
t_2	12	3	0.5	15	15	0.4	**0.0513**
t_3	11	8	1	20	15	0.5	**0.0711**
t_4	15	4	1	25	15	0.6	**0.0354**
t_5	15	4	1.5	28	15	0.65	**0.0322**

TABLE VI
Parameters for a Wildfire Approaching Overhead Conductors A-B1-C2 and the Associated Time-Variant Failure Likelihood

Time	Physical Features/Environmental Features						P(Failure)
	S (°)	M_s (%)	F_D (cm)	V_w (km/h)	h (m)	L_f (m)	
t_1	-5	15	4	10	15	0.5	**0.4180**
t_2	-4	20	3.5	15	15	0.6	**0.4817**
t_3	-2	25	3	20	15	0.75	**0.5401**
t_4	-3	30	2	25	15	1	**0.7239**
t_5	-1	25	2	40	15	1.5	**0.6618**

VI. Conclusion

Power distribution networks in general and overhead power line conductors in particular are vulnerable to wildfires, jeopardizing the operation reliability in supplying energy to end-use customers. Given the hazard intensity, fragility curves are commonly used in the literature to analyze the equipment failure likelihood in order to estimate the vulnerability of power delivery infrastructure and the system performance reliability. However, since power distribution lines run through wide geographical areas with varying vegetation coverage, establishing a fragility curve that precisely describes the likelihood of failure for each individual conductor is time expensive and practically not viable. This article first characterized the wildfire behaviour approaching the power delivery infrastructure and then modeled its influence on the temperature rise of the overhead ACSR-type power line conductors. Accordingly, a parameterized wildfire fragility function, for the first time, was proposed for overhead power line conductors when facing wildfire incidents. The suggested fragility model is function of a set of influencing (competing or supporting) factors including 1) land slope, fuel aridity index, fuel depth, conductor height (*physical features*), 2) fire path length, angle between fire and conductor, and air heat coefficient (*fire features*), and 3) wind speed and flame length (*environmental features*). To assess the likelihood of conductor failure in the face of an approaching wildfire, the Halton quasi-random points methodology was utilized to generate 20,000 training sample points for the physical and environmental parameters, while the LHS method was employed to generate 20,000 random realizations for the fire parameters. Based on the generated samples, a logistic regression model was used to construct a closed-form expression for the conductor likelihood of failure. The numerical results demonstrated that the proposed parameterized wildfire fragility function could offer the likelihood of failure for each individual overhead conductor more precisely than the conventional two-dimensional fragility curves commonly used in the literature. The proposed parameterized wildfire fragility function can assist electric power distribution utilities in investigating power lines physical vulnerability in the face of progressing wildfires, evaluating replacement options, and determining the most cost-effective hardening practices to achieve a more resilient power distribution network against future wildfires.

Appendix A
Convective Heat Equation

According to [34], the convective heat gained by overhead power line conductors that are exposed to a progressing wildfire can be expressed as follows.

$$Q_c = C_f.(T - T_a) = f.\Delta T_a = 22.C_f.\frac{\rho^{\frac{2}{3}}}{h^{\frac{6}{3}}}$$

where Q_c denotes the convective heat flux (kW/m^2), C_f reflects the convective heat transfer coefficient ($\frac{kW}{m^2.^\circ K}$), T_a is the ambient temperature (K), ρ indicates the total heat release rate from the source (kW), and h is the conductor height from the ground (m). It should be noted that the convective heat transfer coefficient is always uncertain and its value varies depending on the geometry of the objective, and the fluid's characteristics [4].

Appendix B
Radiative Heat Equations

According to [4], [35], for fires with small to moderate flame length, the radiation heat flux can be estimated as follows:

$$Q_r = \frac{\xi_r.\rho}{4.\pi.R^2},$$

where Q_r indicates the radiative heat flux (kW/m^2), R (m) is the distance between the progressing wildfire and the conductor surface, ξ_r is the radiative fraction of heat that transfers through electromagnetic waves, and ρ represents the overall heat release rate (kW). The value of ξ_r changes from 0.60 for small fires to 0.15 for fires with high intensity with black smokes [34], [35], [36], [37]. In this article, $\xi = 0.40$ is considered for small to moderate wildfires.

A wildfire with angle θ_f is approaching toward an overhead power line conductor of height h. The initial distance of fire from the conductor is considered as $+l/2$ on y axis (see Fig. 1), and the farthest distance between wildfire and the conductor is considered as $-l/2$ at which the wildfire effect on the conductor temperature is approximately zero. The radiative heat flux on the conductor for dx of the fire front can be estimated as follows:

$$Q_{r(dx)} = \frac{0.4.\rho}{4.\pi.R^2} = \frac{0.4.I_B.\cos\theta.dx}{4.\pi.R^2},$$
$$R^2 = h^2 + a^2 = h^2 + \left(x'^2 + y'^2\right).$$

Assuming that the fire front is longer than the line span [4], the total radiative heat flux on the conductor is calculated in the following:

$$Q_{r(dx)} = \frac{0.4.I_B.\cos\theta}{4.\pi}.\int_{-\infty}^{+\infty}\frac{dx'}{h^2 + x'^2 + y'^2}.$$

Considering the wildfire approaches the conductor with the rate of spread γ_f and the distance that fire passes through is from $(+l/2)$ to $(-l/2)$ on the y axis, the radiative heat energy W_r (kJ/m^2) can be presented as follows [4]:

$$\begin{aligned}
W_r &= \frac{0.4.I_B.\cos\theta}{4.\pi}.\int_0^{\frac{l}{\gamma_f}}\int_{-\infty}^{+\infty}\frac{dx'.dt}{h^2 + x'^2 + (\gamma_f.t)^2} \\
&= \frac{I_B.\cos\theta}{10.\pi}.\int_0^{\frac{l}{\gamma_f}}\int_{-\infty}^{+\infty}\frac{dx'.dt}{\lambda^2(t) + x'^2} \\
&= \frac{I_B.\cos\theta}{10.\pi}.\int_0^{\frac{l}{\gamma_f}}\frac{\pi.dt}{\lambda(t)} = \frac{I_B.\cos\theta}{10}.\int_0^{\frac{l}{\gamma_f}}\frac{dt}{\sqrt{h^2 + \gamma_f^2.t^2}} \\
&= \frac{I_B.\cos\theta}{10.\gamma_f}.\ln\left(t + \sqrt{t^2 + \left(\frac{h}{\gamma_f}\right)^2}\right)\Bigg|_0^{l/\gamma_f} \\
&= \frac{I_B.\cos\theta}{10.\gamma_f}.\left[\ln\left(\frac{\frac{l}{\gamma_f}}{\frac{h}{\gamma_f}}\right) + \ln\left(1 + \sqrt{1 + \left(\frac{h}{l}\right)^2}\right)\right]
\end{aligned}$$

TABLE VII
CHARACTERISTICS OF THE BARE ACSR 95 CONDUCTOR [4]

Notation	Definition	Value
$\varkappa_{st}$	Number of Strands of Steel	7
$\varkappa_{Al}$	Number of Strands of Aluminum	26
ς_{st}	Specific Weight of Steel	7800 (kg/m^3)
ς_{Al}	Specific Weight of Aluminum	2700 (kg/m^3)
ω_{st}	Specific Heat Coefficient of Steel	0.502 ($kJ/kg.°C$)
ω_{Al}	Specific Heat Coefficient of Aluminum	1.637 ($kJ/kg.°C$)
δ_{st}	Strand Diameter of Steel	0.00211 (m)
δ_{Al}	Strand Diameter of Aluminum	0.00272 (m)
d_c	External Diameter of the Conductor	0.01724 (m)

TABLE VIII
PERFORMANCE COMPARISON BETWEEN THE PROPOSED FRAGILITY MODEL VS. STATE-OF-THE-ART MODELS

	Proposed Method	Ref [38]	Ref [39]	Ref [40]
Failure Likelihood	0.4180	≤ 0.01	≤ 0.01	≤ 0.01

$$= \frac{I_B.\cos\theta}{10.\gamma_f}.\left[\ln\left(\frac{l}{h}\right)+\ln\left(1+\sqrt{1+\left(\frac{h}{l}\right)^2}\right)\right]$$

APPENDIX C
DEFINITION OF PARAMETERS IN EQUATION (6)

Table VII tabulates the definition and the value of each parameter in (6).

APPENDIX D
PERFORMANCE COMPARISON

The performance of the proposed multi-dimensional wildfire fragility model in this article is compared to the existing one-dimensional wind fragility models in the literature, which primarily consider wind speed as the severity index. To emphasize the significance of the contribution of environmental parameters (e.g., landscape slope, fuel aridity index, etc.), wind speed, which is the most common severity index for existing one-dimensional fragility curves in the literature, is considered to be very low (2.77 m/s). The likelihood of failure for a power line with a height of $h = 15$ m in a landscape with a slope of $S = -5°$, fuel aridity index of $M_s = 15\%$, fuel depth of $F_D = 4$ cm, and assuming the fire length of $L_f = 0.5$ m is shown in Table VIII.

It is evident that relying solely on one-dimensional fragility models, which consider the probability of failure based solely on wind speed, is insufficient for predicting power line failures during wildfires. The findings indicate that even with low wind speeds, factors such as slope, fuel aridity index, fuel depth, and fire characteristics significantly contribute to the likelihood of power line failures during wildfires. The comparison results provide clear evidence that wind intensity alone is inadequate, and it is crucial to consider other environmental parameters for an effective wildfire fragility assessment of power lines.

REFERENCES

[1] Insurance Information Institute (III), Facts statistics: Wildfires, 2020. [Online] Available: https://www.iii.org/fact-statistic/facts-statistics-wildfires
[2] W. M. Jolly et al., "Climate-induced variations in global wildfire danger from 1979 to 2013," *Nature Commun.*, vol. 6, no. 1, pp. 1–11, 2015.
[3] B. Chiu, R. Roy, and T. Tran, "Wildfire resiliency: California case for change," *IEEE Power Energy Mag.*, vol. 20, no. 1, pp. 28–37, Jan./Feb. 2022.
[4] E. I. Koufakis, P. T. Tsarabaris, J. S. Katsanis, C. G. Karagiannopoulos, and P. D. Bourkas, "A wildfire model for the estimation of the temperature rise of an overhead line conductor," *IEEE Trans. Power Del.*, vol. 25, no. 2, pp. 1077–1082, Apr. 2010.
[5] J. R. Harvey, "Effect of elevated temperature operation on the strength of aluminum conductors," *IEEE Trans. Power App. Syst.*, vol. PAS-91, no. 5, pp. 1769–1772, Sep. 1972.
[6] F. Jakl and A. Jakl, "Effect of elevated temperatures on mechanical properties of overhead conductors under steady state and short-circuit conditions," *IEEE Trans. Power Del.*, vol. 15, no. 1, pp. 242–246, Jan. 2000.
[7] G. Beers, S. Gilligan, H. Lis, and J. Schamberger, "Transmission conductor ratings," *IEEE Trans. Power App. Syst.*, vol. 82, no. 68, pp. 767–775, Oct. 1963.
[8] S.-D. Kim and M. M. Morcos, "Mechanical deterioration of ACSR conductors due to forest fires," *IEEE Trans. Power Del.*, vol. 18, no. 1, pp. 271–276, Jan. 2003.
[9] Z. Wang et al., "Prediction of the failure probability of the overhead power line exposed to large-scale jet fires induced by high-pressure gas leakage," *Int. J. Hydrogen Energy*, vol. 46, no. 2, pp. 2413–2431, 2021.
[10] S. D. Anagnostatos, C. D. Halevidis, A. D. Polykrati, E. I. Koufakis, and P. D. Bourkas, "High-voltage lines in fire environment," *IEEE Trans. Power Del.*, vol. 26, no. 3, pp. 2053–2054, Jul. 2011.
[11] L. Zárate, J. Arnaldos, and J. Casal, "Establishing safety distances for wildland fires," *Fire Saf. J.*, vol. 43, no. 8, pp. 565–575, 2008.
[12] M. Nazemi and P. Dehghanian, "Powering through wildfires: An integrated solution for enhanced safety and resilience in power grids," *IEEE Trans. Ind. Appl.*, vol. 58, no. 3, pp. 4192–4202, May/Jun. 2022.
[13] D. N. Trakas and N. D. Hatziargyriou, "Optimal distribution system operation for enhancing resilience against wildfires," *IEEE Trans. Power Syst.*, vol. 33, no. 2, pp. 2260–2271, Mar. 2018.
[14] M. Nazemi, P. Dehghanian, M. Alhazmi, and Y. Darestani, "Resilient operation of electric power distribution grids under progressive wildfires," *IEEE Trans. Ind. Appl.*, vol. 58, no. 2, pp. 1632–1643, Mar./Apr. 2022.
[15] M. Abdelmalak and M. Benidris, "Enhancing power system operational resilience against wildfires," *IEEE Trans. Ind. Appl.*, vol. 58, no. 2, pp. 1611–1621, Mar./Apr. 2022.
[16] A. F. Mensah and L. Dueñas-Osorio, "Efficient resilience assessment framework for electric power systems affected by hurricane events," *J. Struct. Eng.*, vol. 142, no. 8, 2016, Art. no. C4015013.
[17] U. P. Onyewuchi, A. Shafieezadeh, M. M. Begovic, and R. DesRoches, "A probabilistic framework for prioritizing wood pole inspections given pole geospatial data," *IEEE Trans. Smart Grid*, vol. 6, no. 2, pp. 973–979, Mar. 2015.
[18] M. Ouyang and L. Duenas-Osorio, "Multi-dimensional hurricane resilience assessment of electric power systems," *Struct. Saf.*, vol. 48, pp. 15–24, 2014.
[19] Y. M. Darestani and A. Shafieezadeh, "Multi-dimensional wind fragility functions for wood utility poles," *Eng. Struct.*, vol. 183, pp. 937–948, 2019.
[20] Y. Darestani, J. Padgett, and A. Shafieezadeh, "Parametrized wind–surge–wave fragility functions for wood utility poles," *J. Struct. Eng.*, vol. 148, no. 6, 2022, Art. no. 04022057.
[21] A. Shafieezadeh, U. P. Onyewuchi, M. M. Begovic, and R. DesRoches, "Age-dependent fragility models of utility wood poles in power distribution networks against extreme wind hazards," *IEEE Trans. Power Del.*, vol. 29, no. 1, pp. 131–139, Feb. 2014.
[22] Ø. R. Solheim, T. Trötscher, and G. Kjølle, "Wind dependent failure rates for overhead transmission lines using reanalysis data and a Bayesian updating scheme," in *Proc. IEEE Int. Conf. Probabilistic Methods Appl. Power Syst.*, 2016, pp. 1–7.
[23] N. Bhusal, M. Gautam, M. Abdelmalak, and M. Benidris, "Modeling of natural disasters and extreme events for power system resilience enhancement and evaluation methods," in *Proc. Int. Conf. Probabilistic Methods Appl. Power Syst.*, 2020, pp. 1–6.

[24] S. Dunn, S. Wilkinson, D. Alderson, H. Fowler, and C. Galasso, "Fragility curves for assessing the resilience of electricity networks constructed from an extensive fault database," *Natural Hazards Rev.*, vol. 19, no. 1, 2018, Art. no. 04017019.
[25] P. M. Fernandes, H. S. Botelho, F. C. Rego, and C. Loureiro, "Empirical modelling of surface fire behaviour in maritime pine stands," *Int. J. Wildland Fire*, vol. 18, no. 6, pp. 698–710, 2009.
[26] A. Polykrati, C. Karagiannopoulos, and P. Bourkas, "Thermal effect on electric power network components under short-circuit currents," *Electric Power Syst. Res.*, vol. 72, no. 3, pp. 261–267, 2004.
[27] L. Kocis and W. J. Whiten, "Computational investigations of low-discrepancy sequences," *ACM Trans. Math. Softw.*, vol. 23, no. 2, pp. 266–294, 1997.
[28] J. C. Helton and F. J. Davis, "Latin hypercube sampling and the propagation of uncertainty in analyses of complex systems," *Rel. Eng. Syst. Saf.*, vol. 81, no. 1, pp. 23–69, 2003.
[29] V. J. Romero, J. V. Burkardt, M. D. Gunzburger, and J. S. Peterson, "Comparison of pure and "latinized" centroidal voronoi tessellation against various other statistical sampling methods," *Rel. Eng. Syst. Saf.*, vol. 91, no. 10/11, pp. 1266–1280, 2006.
[30] D. Doss, "Primer on ACSS/TW overhead conductor," *POWERGRID Int. Publication Mag.*, [Online] Available: https://www.power-grid.com/td/primer-on-acss-tw-overhead-conductor/#gref
[31] "ACSR overhead conductor data sheet," [Online] Available: http://www.alfasanat.com/en/alfacable/Products/57-Bare_Overhead_Conductors__ACSR_/
[32] G. P. Balomenos, S. Kameshwar, and J. E. Padgett, "Parameterized fragility models for multi-bridge classes subjected to hurricane loads," *Eng. Struct.*, vol. 208, 2020, Art. no. 110213.
[33] Y. M. Darestani, B. Webb, J. E. Padgett, G. Pennison, and E. Fereshtehnejad, "Fragility analysis of coastal roadways and performance assessment of coastal transportation systems subjected to storm hazards," *J. Perform. Constructed Facilities*, vol. 35, no. 6, 2021, Art. no. 04021088.
[34] D. Drysdale, *An Introduction to Fire Dynamics*. Hoboken, NJ, USA: Wiley, 2011.
[35] D. J. Icove and J. D. DeHaan, "Fire scene reconstruction," *Fire Protection Eng.*, vol. 21, pp. 10–16, 2004.
[36] J. D. DeHaan et al., *Kirk's Fire Investigation*. New York city, NY, USA: Pearson Higher Ed., 2011.
[37] J. G. Quintiere, *Principles of Fire Behavior*. Boca Raton, FL, USA: CRC, 2016.
[38] X. Fu, H.-N. Li, G. Li, Z.-Q. Dong, and M. Zhao, "Failure analysis of a transmission line considering the joint probability distribution of wind speed and rain intensity," *Eng. Struct.*, vol. 233, 2021, Art. no. 111913.
[39] M. Panteli, C. Pickering, S. Wilkinson, R. Dawson, and P. Mancarella, "Power system resilience to extreme weather: Fragility modeling, probabilistic impact assessment, and adaptation measures," *IEEE Trans. Power Syst.*, vol. 32, no. 5, pp. 3747–3757, Sep. 2017.
[40] J. W. Muhs, M. Parvania, H. T. Nguyen, and J. A. Palmer, "Characterizing probability of wildfire ignition caused by power distribution lines," *IEEE Trans. Power Del.*, vol. 36, no. 6, pp. 3681–3688, Dec. 2021.

Mostafa Nazemi (Member, IEEE) received the B.Sc. degree in electrical engineering from the K. N. Toosi University of Technology, Tehran, Iran, in 2015, the M.Sc. degree in energy systems engineering from the Sharif University of Technology, Tehran, Iran, in 2017, and the Ph.D. degree in electrical engineering from The George Washington University, Washington, DC, USA, in 2022. He is an Electrical Engineer with MPR Associates, Inc. His research interests include power system resilience, power system planning and operation, energy optimization, and smart electricity grid applications. Dr. Nazemi was the recipient of the 2018 Certificate of Excellence in Reviewing by the Editorial Board Committee of the Journal of Modern Power and Clean Energy.

Payman Dehghanian (Senior Member, IEEE) received the B.Sc. in electrical engineering from the University of Tehran, Tehran, Iran, in 2009, the M.Sc. degree in electrical engineering from the Sharif University of Technology, Tehran, in 2011, and the Ph.D. degree in electrical engineering from Texas A&M University, College Station, TX, USA, in 2017. He is currently an Associate Professor with the Department of Electrical and Computer Engineering, George Washington University, Washington, DC, USA. His research interests include power system reliability and resilience assessment, data-informed decision-making for maintenance and asset management in electrical systems, and smart electricity grid applications. Dr. Dehghanian was the recipient of the 2014 and 2015 IEEE Region 5 Outstanding Professional Achievement Awards, 2015 IEEE-HKN Outstanding Young Professional Award, 2021 Early Career Award from the Washington Academy of Sciences, and 2022 Early Career Researcher Award from the George Washington University.

Yousef Darestani received the B.Sc. in civil engineering from the University of Tehran, Tehran, Iran, in 2011, the M.Sc. degree in structural engineering from Sharif University of Technology, Tehran, in 2014, and the Ph.D. degree in civil engineering from the Ohio State University, Columbus, OH, USA, in 2019. He is currently an Assistant Professor with the Department of Civil, Environmental, and Geospatial Engineering, Michigan Technological University, Houghton, MI, USA. His research interests include risk, reliability, and resilience assessment and enhancement of infrastructure systems against natural hazards.

Jinshun Su (Graduate Student Member, IEEE) received the B.Eng in electrical engineering from Xi'an University of Technology, Xi'an, China in 2017, and the M.Sc. degree in electrical engineering from The George Washington University, Washington, DC, USA in 2019. He is currently working toward the Ph.D. degree in electrical engineering with the Department of Electrical and Computer Engineering, George Washington University. His research interests include applications of mobile power sources for resilient smart grids, as well as modeling and analysis of decision-dependent uncertainties in energy system's decision-making processes.